Arab J Sci Eng (2012) 37:2127–2136
DOI 10.1007/s13369-012-0302-6

RESEARCH ARTICLE - CIVIL ENGINEERING

Isfendiyar Egeli · Handan Usun

Designing High-Speed Train Railway Embankments Using Finite Element Analysis

Received: 13 August 2010 / Accepted: 13 March 2011 / Published online: 15 May 2012

Abstract Design and construction of high-speed train railway (HSTR) infrastructure is different from that for normal trains, since high geometric standards and material properties are involved. For example, HSTR embankments are designed to limit total-differential settlements to minute amounts. In this study, a typical 'slab-track' type HSTR embankment was used to investigate the replaceability of one fill strata known as 'uncemented-prepared-subgrade layer' (U-PSL), constructed by using a locally obtained medium sand, as opposed to various 'cemented-prepared-subgrade layers' (C-PSL), whose mixes were prepared at two water-to-cement (w/c) ratios and three cement contents (c). Three size cylindrical samples were cast, 7–28 days water cured and were tested to obtain the unconfined compressive stresses, strains, elasticity moduli and Poisson's ratios at failure. Test results were then fed into the Plaxis-FEM program to find the maximum total settlements of individual layers and compared with the requirements. Only three C-PSL mixes having cement contents (c) of 20, 25, 30 % and water-to-cement (w/c) ratios of 0.4 and 0.5 met the strict settlement criteria. The study showed that the original ($h = 2$ m) thick U-PSL can be replaced with $0.3h$-m thick C-PSL at w/c = 0.5 (i.e. $h = 0.6$ m). Likewise, the original ($h = 2$ m) thick U-PSL can be replaced with $0.2h$-m thick C-PSL at w/c = 0.4 (i.e. $h = 0.4$ m). Also, the extra effort of doing in situ soil compaction and testing in layers is reduced or eliminated. This would give not only alternative ways to HSTR embankment designers/constructors, but also substantial savings in construction time and costs.

Keywords High-speed trains railways · Embankment design · Fill settlements

الخلاصة

إن البنية التحتية لقطار فائق السرعة للسكك الحديدية (HSTR) تختلف عن تلك التي للقطارات العادية، لتضمنها معايير هندسية عالية الجودة ومواد خاصة. فقد تم - على سبيل المثال - تصميم سدود لقطار HSTR لتلبية الفروق الكلية الدقيقة للمستوطنات. وفي هذه الدراسة تم استخدام جسر نموذجي نوعه "لوح المسار" HSTR للتحقيق في إمكانية استبدال طبقة ملء تسمى طبقة الأرض الطبيعية المُعدّة غير المعززة (U-PSL) مع واحدة معززة تسمى"C-PSL"، وذلك باستخدام الرمل المتوسط المحلي وإعداد عينات اختبار إسطوانية ثلاثية الحجم مع نسبة الماء/الأسمنت 2 ومحتوى إسمنت 3 التي تم اختبار مواطن قوة الضغط غير المحصورة فيها بعد 28 يوما من الشفاء للحصول على نسب الإجهاد/ السلالة/معاملات المرونة/بواسون عند الفشل. لقد تم تغذية نتائج الاختبار في برنامج FEM-Plaxis للعثور على الحد الأقصى لمجموع المستوطنات للطبقات الفردية. ثلاث فقط من خلطات PSL-C 3 لها محتوى إسمنت بنسب 20 و 25 و 30٪ مع نسب ماء/إسمنت 0.5 و 0.4 وافقت معايير التسوية الصارمة. وقد أظهرت الدراسة أن حوالي 30٪ من السماكة الأصلي (أي ع = 0.6 م) يمكن أن يُستخدم مع نسبة ماء/إسمنت تساوي 0.5 أو حوالي 20٪ من السماكة الأصلي (أي ع = 0.4 م) يمكن أن يستخدم مع نسبة ماء/إسمنت تساوي 0.4 بدلا من 2م، وهو سمك U-PSL المعتاد الذي ينبغي أن يضغط ويختبر في الطبقات. وسوف يمنح استبدال من هذا القبيل PSL-C وسيلة بديلة لمصممي/ صانعي جسر HSTR، مما قد يعني وجود بعض التوفير في تكاليف البناء.

I. Egeli (✉)
Civil Engineering Department, Izmir Institute of Technology, 35430 Urla-Izmir, Turkey
E-mail: isfendiyaregeli@iyte.edu.tr

H. Usun
Kosuyolu Cad. No: 143/8, Göksel Apt., 35160 Şirinyer-İzmir, Turkey
E-mail: handan_usun@hotmail.com

1 Introduction

Safe, fast, comfortable, affordable, sustainable and environmentally friendly electrical-locomotive driven high-speed train railway (HSTR) travel is becoming more and more popular in today's world in the last few decades. More countries, such as the USA, the Kingdom of Saudi Arabia, Qatar and the UAE have either recently announced plans to develop or have already proceeded to develop this mode of travel to join the privileged club of a few countries, such as France, Spain, Germany, Italy, the UK, Japan, China, Korea and Taiwan, who are already utilizing such travel networks. The definition of high-speed varies from country to country globally, as there is no single standard accepted worldwide. Generally speaking, it is defined as a railway travel service, which regularly operates at a minimum speed of 250 km/h on new tracks, or at a minimum speed of 200 km/h on existing tracks. However, nowadays it has become a norm in countries that use this technology to define 'high-speed' as 'design speeds near and above 400 km/h' [1]. In addition, another definitive aspect of the high-speed rail service is the presence of continuously welded rails in the railway infrastructure. Although, the adopted 'railway gauge' (i.e. the distance between the symmetry axes of two parallel rails in a high-speed train railway (HSTR) differs from country to country, for some countries (including Turkey), the used railway gauge is 1.435 m [2–4]. On the other hand, a 'rail-track' term is used as an engineering unit for a multi-layered composite system, comprised of various layers, increasing in stiffness from natural ground up to the rail level [5]. Because of the high speeds adopted for design, construction and operation, there are strict 'top-of-rail' total-differential settlement requirements in a HSTR embankment, in both the lateral and longitudinal directions. Thus, HSTR embankments are constructed to be much stiffer than those for normal trains. In the Far-Eastern design practice, these layers from bottom to top in sequence are as follows: natural ground (i.e. natural subgrade layer), subgrade layer (artificial), prepared-subgrade layer (PSL), bearing base layer, slab-track layer of unreinforced concrete, reinforced concrete traverses and then rails, connected to the traverses with steel fasteners, as shown in Fig. 1 [6].

2 Properties of the Prepared-Subgrade Layer (PSL) in a HSTR Embankment

(a) Material Properties
In the Far-Eastern design practice, the prepared-subgrade layer (PSL) is located between the bearing-base layer and the (artificial) subgrade layer. The function of the PSL is to minimize deformation of the earthwork layers above and to prevent percolation of water into the earthwork layers below. The

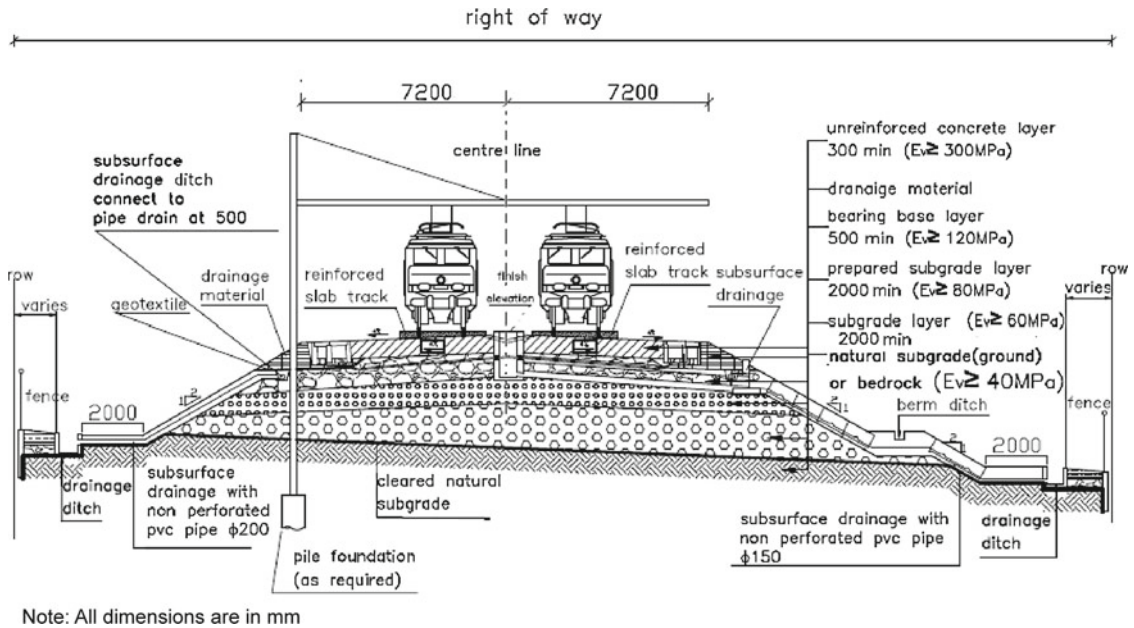

Fig. 1 Cross-section of a 'slab-track' type HSTR embankment as used in the Far-East. (Prepared-subgrade layer is represented by *small dots* in the middle)

Table 1 Recommended gradation envelope of a PSL material in a HSTR embankment

Grain size	Percentage passing
$P(2D)$	100
$P(D_{max})$	100–99
$P(D)$	99–85
$P(D/2)$	84–55
$P(D/5)$	60–31
$P(D/10)$	49–23
$P(D/20)$	40–17
$P(D/50)$	31–11
$P(D/100)$	22–8
$P(D/200)$	16–6
$P(D/500)$	9–3
$P(D/1{,}000)$	6–2

D nominal grain size, D_{max} $1.25D$, if $D \geq 50$ mm; $D_{max} = 1.58D$, if $D < 50$ mm

recommended gradation envelope for a PSL (also called the Uncemented-PSL or U-PSL) material is given in Table 1 [6].

(b) Bearing Capacity and Compactness

The properties of a PSL material is defined by the following standard tests [6]:

- The Standard Proctor Test (ASTM D 698-00) to determine the maximum dry density (MDD) and the optimum moisture content (OMC),
- The Plate Bearing Test (ASTM D 1196-93, 2004), where the maximum particle size is less than 100 mm.

The required critical values for the above mentioned tests are as follows [6]:
The Relative Compaction with respect to MDD from the Standard Proctor Test ($\rho_d \geq 95\,\%$ MDD),
The (vertical) Elasticity Modulus from the Plate Bearing Test ($E \geq 80$ MPa).

2.1 Laboratory Tests for a PSL with Uncemented and Cemented Turgutlu Sand

2.1.1 Laboratory Tests on Uncemented Turgutlu Sand used as U-PSL (PART 1)

In this section, some basic index tests were performed using a locally obtained medium Turgutlu Sand, as it has met the requirements of a typical PSL material [6]. These include the following:

- The particle size analysis (ASTM D422-63, 2005),
- The compaction test, using the standard proctor method (ASTM D698-00, 2005),
- The specific gravity test (ASTM D854-02, 2005),
- The water content test (ASTM D2216, 2005),
- Soil classification method by using the unified soil classification system-USCS (ASTM D2487-00, 2005),
- The consolidated-drained (CD) triaxial test (ASTM WK3821, 2005),
- The direct shear test (ASTM D3080-04, 2005),
- The unit weight of soils test (ASTM D4253-00, 2005) and
- The permeability test (ASTM D 2434-68, 2006). A brief summary of tests is given below.

(a) Particle Size Analysis

This test was applied to determine the variation of different grain sizes, contained within a soil specimen. Sieve analysis was performed to determine the distribution of the particle sizes. Test standard used was ASTM D 422-63, 2005-'Standard Test Method for Particle Size Analysis of Soils'. This and other test results are given in Table 2 [12].

(b) The Laboratory Compaction Test

For this test, the ASTM D 698-00, 2005-'Standard Test Method for Laboratory Compaction Characteristic of Soil Using Standard Compaction Effort' method was used. The obtained results are as follows [12]:

- The Optimum moisture content, (%), $W_{opt.} = 13.6$.
- The Maximum dry density, (kN/m^3), $\gamma_{drymax.} = 19.994$.

Table 2 Summary of laboratory tests results of uncemented-Turgutlu Sand used as U-PSL

No.	Experiment name	Used method	ASTM-D	Value	Unit
1	Particle size analysis	Wet sieve analysis	ASTM-D 422-63	–	(%)
2	The laboratory compaction test	Standard Proctor method	ASTM-D 698-00	W_{opt} = 13.6, γ_{drymax} = 19.994	(%) kN/m^3
3	Specific gravity of soil solids	Pycnometer method	ASTM-D 854-02	2.65	–
4	Determination of water content	Oven dried method	ASTM-D 2216	(3.3%) in laboratory conditions	(%)
5	Classification of soil for engineering purposes	USCS	ASTM-D 2487-00	SP	–
6	Coefficient of permeability	Falling head method	ASTM-D 5084-03	10^{-3}	m/s
7	Maximum index density	Vibration table method	ASTM-D 4253-00	–	–
8	Triaxial compression test	Consolidated-drained (CD)	ASTM WK3821	c = 7, Ø = 37	kPa (°)
9	Direct shear test	Consolidated-drained (CD)	ASTM-D 3080-04	c = 7, Ø = 36.88	kPa (°)

Table 3 Design values for the prepared mixes of cemented-Turgutlu Sand used as C-PSL

No.	Name	Value	Unit
1	Slump	70	mm
2	Max size of aggregate	50	mm
3	Mixing water and air content	Depends on w/c	–
4	Water/cement ratio (w/c)	0.4–0.5	–
5	Cement content	10, 15, 20, 25, 30	(%) By weight of concrete
6	Coarse aggregate content	Depends on w/c	–

2.1.2 Laboratory Tests on Cemented-Turgutlu Sand used as C-PSL (PART 2)

In these tests, type-1 Portland cement (ASTM C150, 1994) and local medium Turgutlu Sand was used for finding the right mix proportions at two water-to-cement ratios (w/c = 0.4, 0.5) and with five cement contents (c = 10, 15, 20, 25, 30 %). Then, three different sizes (based on diameter and height values) of cylindrical steel molds were used to cast the prepared samples to be water cured for 7 and 28 days, before testing them in the unconfined compression test machine at the IYTE-MAM Laboratory to obtain their uniaxial compressive strengths (per local standards: TS EN 12390-2, 2002; -3, 2003) [7–11]. The adopted design values for the prepared mixes of Cemented-Turgutlu Sand used as C-PSL are given in Table 3 [12].

Three cylindrical specimens were cast for the (small) sample A-size (diameter, $D = 4$ cm and length, $L = 8$ cm), another three specimens were cast for the (medium) sample B-size (diameter, $D = 8$ cm, length, $L = 16$ cm) and a separate three specimens were cast for the (large) sample C-size (diameter, $D = 10$ cm, length, $L = 20$ cm). There were three specimens in each of 30 sets, making altogether 90 specimens in each one of three (size: A, B, C) groups, making altogether 270 specimens with the C-PSL material [12]. The first specimen in each set was tested, after 7 days of water-curing and the other two were tested, after 28 days of water-curing. In each group, there were samples having five different cement contents (c = 10, 15, 20, 25, 30 %) with two different water-to-cement ratios (w/c = 0.4 and 0.5). Of these 270 specimens, 90 numbers (30 numbers for each of three sizes) were tested after 7 days of water curing and the remainder 180 numbers (60 numbers for each of three sizes) were tested after 28 days of water-curing for determining their unconfined compressive strengths. In these tests, the Universal Testing Machine at the IYTE-MAM Laboratory was used. Area correction was applied and the largest compressive force reached during the compression process was taken as the break force and used in the subsequent analyses [12].

2.1.3 Evaluation of Laboratory Test Results with Turgutlu Sand

The evaluation of the results of the Unconfined Compression tests conducted on the cemented-prepared-subgrade layer (C-PSL) specimens were studied from two different viewpoints, as detailed below.

(a) Evaluation of Elasticity Moduli Results for 28-day cured C-PSL specimens
(a1) For the 28-day cured specimens having w/c = 0.5, the increase of Elasticity Modulus (E) versus cement content (c) were almost linear, though slope was greater for the small (A-size), than the large (C-size) specimens, where the correlation coefficients were high ($0.9 < R^2 < 1.0$) and medium ($0.8 < R^2 < 0.9$), respectively. For the medium (B-size) specimens, E increased exponentially faster

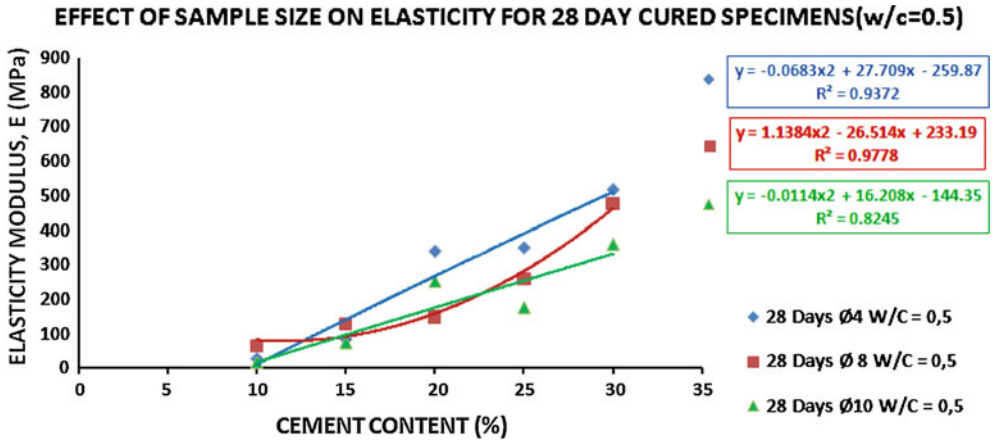

Fig. 2 Effect of sample size on Elasticity Modulus for 28-day cured specimens (w/c = 0.5)

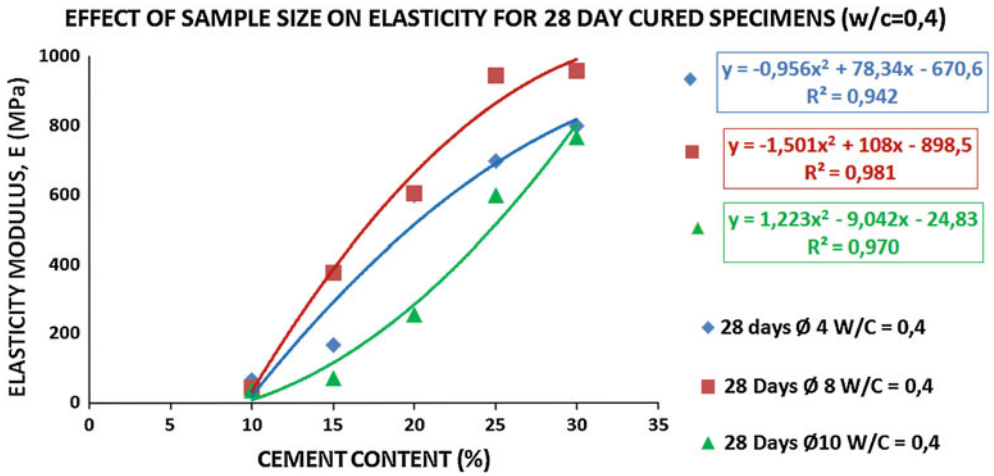

Fig. 3 Effect of sample size on elasticity modulus for 28-day cured specimens (w/c = 0.4)

with the cement content. It is noted that if the variation increases faster exponentially with an upward curvature, it is considered to show a positive curvature, as displayed by B-size in Fig. 2 [12]. On the other hand, if the variation increases exponentially slower with downward curvature, it is considered to show a negative curvature, as displayed by small (A) and medium (B) sizes in Fig. 3, where all sizes had high correlation coefficients.

(a2) For 28-day cured specimens having w/c = 0.4, the values of Elasticity Moduli (E) were generally higher, compared to those of w/c = 0.5. Furthermore, the increase in E with respect to cement content (c) was higher for small (A-size) specimens, than for medium (B-size) specimens, which were in turn higher than for the large (C-size) specimens. Though the first two displayed E increasing exponentially slower trend (with negative curvature) as a function of cement content (c), the last one displayed E increasing exponentially faster trend (with positive curvature) as a function of cement content (c), as seen in Fig. 3 [12].

(b) Evaluation of Compressive Strength Results for 28-day cured C-PSL specimens

(b1) For the 28-day cured specimens having w/c = 0.5, an increase in Compressive Strength with respect to cement content (c) showed a linear-like relationship for both small (A-size) and large (C-size) specimens, compared to medium (B-size) specimens, which displayed increasing faster exponentially trend with positive curvature. Though the first two had high correlation coefficients, the last one had medium correlation coefficient, as seen in Fig. 4 [12].

(b2) For the 28-day cured specimens having w/c = 0.4, values of compressive stress at failure (i.e. Compressive Strength) as a function of cement content (c) were generally higher, compared to those of w/c = 0.5. Furthermore, Compressive Strength's increase with cement content (c) was higher for

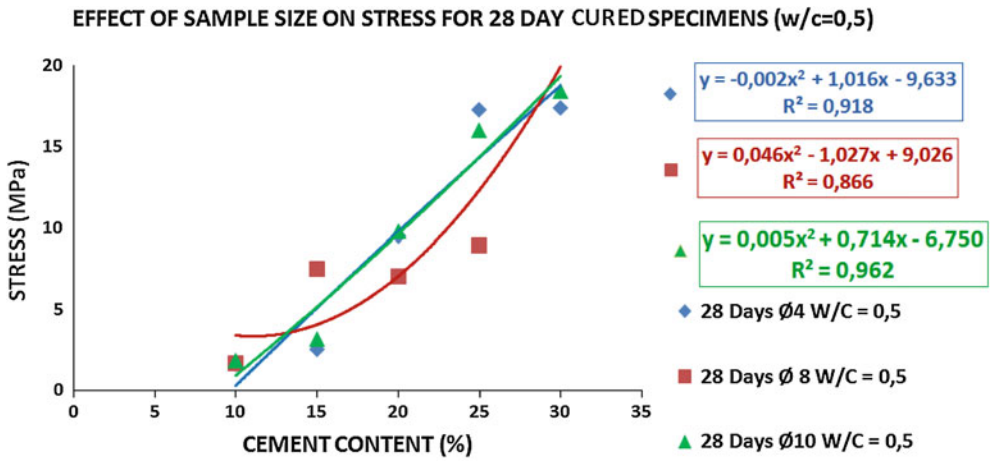

Fig. 4 Effect of sample size on compressive strength for 28-day cured specimens (w/c = 0.5)

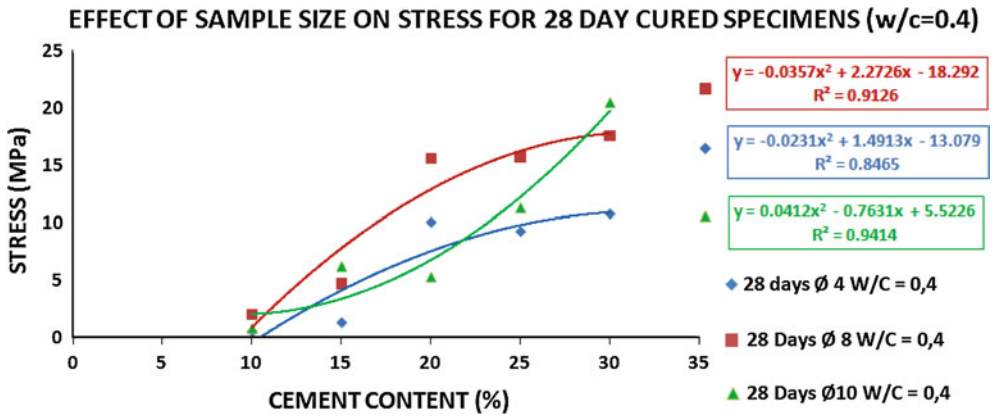

Fig. 5 Effect of sample size on compressive strength for 28-day cured specimens (w/c = 0.4)

medium (B-size) specimens, compared to those for small (A-size) and large (C-size) specimens up to c = 30 %. Though the first two had increased exponentially slower with negative curvature, the last one had increased exponentially faster with positive curvature. For small (A-size) samples, the correlation coefficient was medium, but for the other (B- and C-size) samples, correlation coefficients were high, as shown in Fig. 5 [12].

2.1.4 Analysis of a HSTR Embankment Settlements

The term 'settlement' here refers to the total and differential settlements at the 'top of rail', including those contributed by the embankment's natural subgrade layer (i.e. the base-ground) and by various embankment layers above the base-ground, but below the traverses.

The elastic deformation of the track-bed is an essential characteristic of the conventional rail-track structure. It enables a load distribution to take place from the wheels, via rails, to a number of traverses. Consequently, if the track-bed with its underlying various embankment layers are all too stiff, this situation may cause higher load concentrations and increased abrasions in the gravel of the ballast layer. This, in turn, may create locally different stiffness and may yield to differential rail deformations under the rail's traffic loads. These differential rail deformations can cause adverse rearrangement of dynamic wheel forces, which, in the end, may lead to progressive worsening of the rail geometry, thus yielding to accelerated wheel/rail and rail/traverse wear and tear. That is why carrying out routine weekly and monthly maintenance/checks are very important (e.g. regular checking of rail conditions for existence of any tiny cracks). In addition, rail connections and 'top of rail' settlements should be checked during the regular maintenance periods. Some new equipment, which uses ultrasound as well as laser technology exists and is mounted inside or outside on the front or back side

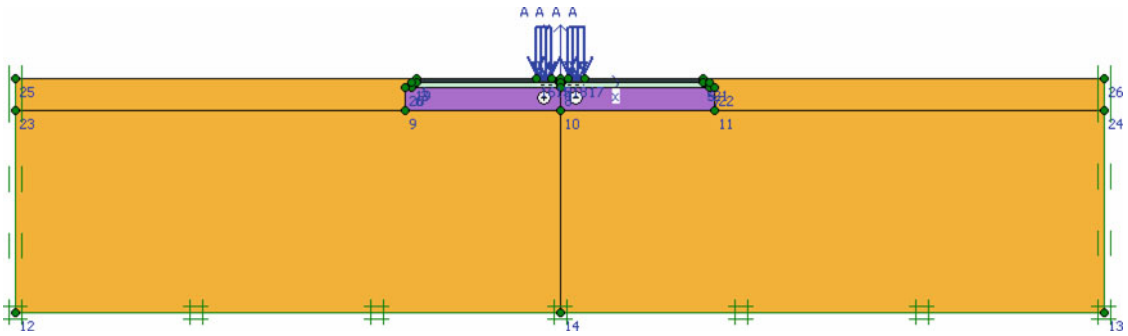

Fig. 6 HSTR embankment model used in this study

of a maintenance locomotive, to allow these checks to be done quickly, while the train moves at a minimum speed of 100 km/h. Thus, it is important to provide and maintain an optimum 'rail-track' structure to avoid excessive/detrimental rail settlements, since each layer's settlement is added-up from the bottom to the top, to constitute the total settlement measured at the 'top of rail' level. Hence, it is important that over the long-term (usually 30 years), the maximum top-of-rail settlements stay within the tolerable limits. Otherwise, excessive total and differential settlements may affect stability and safety of the ride with high-speed trains (HST), apart from causing fast condition deterioration in the HST wheels and in its infrastructure. That's why nowadays HST infrastructure-designers have to decide between the two very distinct infrastructure types, used mostly in the Europe or in the Far-East.

The general European practice of using 'ballast-supported-rail-tracks' are less costly to built, but more difficult and costly to maintain in the long term, though it is easier to do track repairs to bring occurred total settlements to tolerable values, because of the frequent re-leveling that can be done easily, during any routine monthly or seasonal maintenance. On the other hand, the Far-Eastern practice of using reinforced concrete 'slab-track' type paved rail-tracks are more costly to built, but easier and cheaper to maintain in the long term, though this type is more difficult and costly to repair/maintain later over a long term to bring occurred total settlements to be within the allowable limits, if they have undergone excessive settlements. The criterion for the maximum allowable (tolerable) total settlement value (ASV or Δs) for any 20-m long longitudinal section of a HSTR embankment in the long term of 30 years after construction is almost the same for both the 'ballasted' and 'slap-track' cases $\Delta s \leq 10$ mm for a HST speeding between 200 and 400 km/h [6].

On the other hand, according to Far-Eastern design practice, the criterion for the maximum tolerable total and differential settlements in the lateral (transverse) direction of the embankment ($\Delta s_{transverse}$) is limited for the same speed range to $\Delta s_{transverse} \leq 2$ mm [6].

2.1.4.1 Methodology for Settlement Analyses of HSTR Embankments In this section, a HSTR embankment model and analysis as obtained by using the Plaxis V8 (2D) FEM program is explained as follows:

1. First of all, a HSTR embankment is modeled as shown in Fig. 6 [12].
2. There are three more HSTR embankment layers above the natural subgrade, which are from top to bottom: the unreinforced 'slab-track' layer, 'bearing-base' layer, 'uncemented- or cemented-prepared subgrade layer (U-PSL or C-PSL, whichever is used), and the (artificial) 'subgrade layer', as seen in Fig. 1. All of these layers have different material properties. Thus, such individual material properties and test conditions should be separately considered and introduced into the Plaxis-FEM Program used. It was considered that traverses and rail connections are rigid and do not contribute to the 'top-of-rail' total settlements computed. The adopted material properties of the individual embankment layers used in this study are given in Table 4 [12].
3. Then a finite element mesh was generated for the used HSTR embankment model, as seen in Fig. 7 [12]. When the initial conditions were assessed and were entered into the Plaxis-FEM program to do settlement analyses, the Ground Water Table was not considered to exist for simplicity. Analyses were made using six experimentally obtained C-PSL elasticity moduli (E) values shown in Table 5 and another analysis was made with $E = 80$ MPa value of U-PSL for comparison purposes [12].
   The variables used in Table 5 were as follows:
   Two water-to-cement ratios (w/c = 0.4, 0.5) and three cement contents (c = 20, 25, 30 %). Although two tests were done for lower cement contents (c) of 10 and 15 %, these were excluded, since they did not

Table 4 Adopted Material Properties for the HSTR embankment model used

Parameter	Name	Unit	Slab track layer	Bearing base layer	Prepared subgrade layer	Subgrade layer
Material model	Model	–	Mohr–Coulomb	Mohr–Coulomb	Mohr–Coulomb	Mohr–Coulomb
Type of material behavior	Type	–	Drained	Drained	Drained	Drained
Soil unit weight above phreatic level	γ_{unsat}	kN/m^3	19	18	17	16
Soil unit weight below phreatic level	γ_{sat}	kN/m^3	22	21	20	19
Permeability in horizontal direction	k_x	m/s	0.2	0.03	0.001	0.00001
Permeability in vertical direction	k_y	m/s	0.2	0.03	0.001	0.00001
Young's modulus	E_{ref}	kPa	300000	120000	80000[a]	60000
Poisson's ratio	ν	–	0.40	0.35	0.30	0.2
Cohesion	c_{ref}	kPa	1	1,5	7	5
Friction angle	Ø	○	40	38	37	35
Dilatancy angle	ψ	○	–	–	2	–

[a] This 80 MPa value is for the uncemented-prepared-subgrade layer, U-PSL

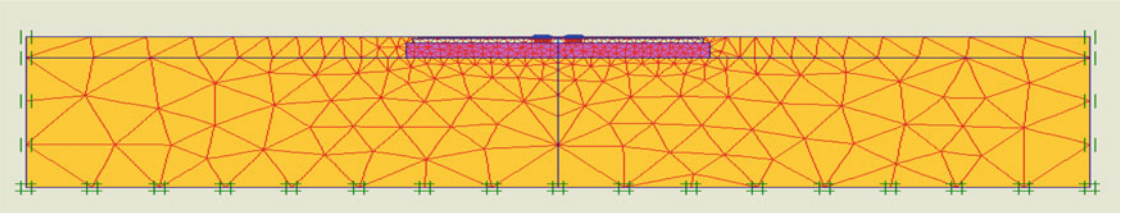

Fig. 7 Generated FEM-mesh of the used HSTR embankment model

Table 5 Variation of C-PSL Elasicity Moduli values with water-to-cement ratios (w/c) and cement contents (c) and their comparison with the minimum $E = 80$ MPa value of U-PSL

w/c ratio	Elasticity modulus, E (MPa) Cement content, c (%)		
	20	25	30
0.5	258.94	261.46	450.47
0.4	352.86	545.20	597.48

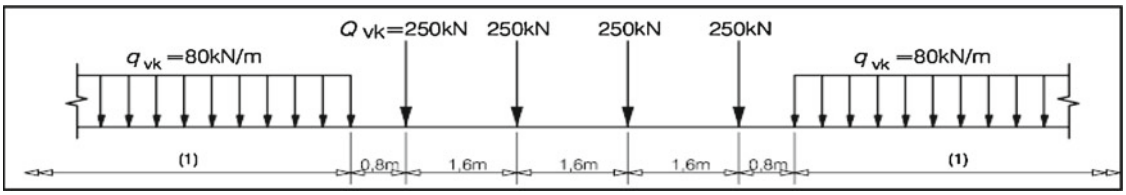

Fig. 8 Load Model 71 and vertical loads in the longitudinal direction of a HSTR embankment

meet the criteria of not-exceeding the total settlement result obtained from the $E = 80$ MPa value of the uncemented-prepared-subgrade layer (U-PSL) used in the Far-East [6,12].

4. For the loading, two general models exist for calculation of the associated static loading effects mentioned in the EN 1991-2: Eurocode 1 [13], where the rail traffic loading is defined by means of load models. Rather than using the Load Model 71 given in Fig. 8, a more critical (causing higher settlement values) Load Model SW/0, given in Fig. 9 and Table 6 was used, in order to better represent static effect of vertical loading, due to normal rail traffic on mainline railway embankments [12].
   The characteristic distances taken for vertical loads of Fig. 8 are given in Table 6 [12].
5. Finally, total settlements that were calculated via the Plaxis-FEM Program using the same six laboratory obtained elasticity moduli (E) values of C-PSL listed in Table 5 and were compared with that of the

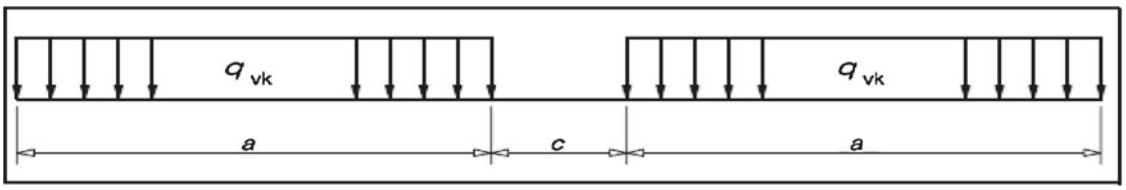

Fig. 9 Load Model SW/0 and vertical loads in the longitudinal direction of a HSTR embankment

Table 6 Characteristic values of the vertical loads for Load Model SW/0

Load model	qvk (kN/m)	a (m)	c (m)
SW/0	133	15.0	5.3

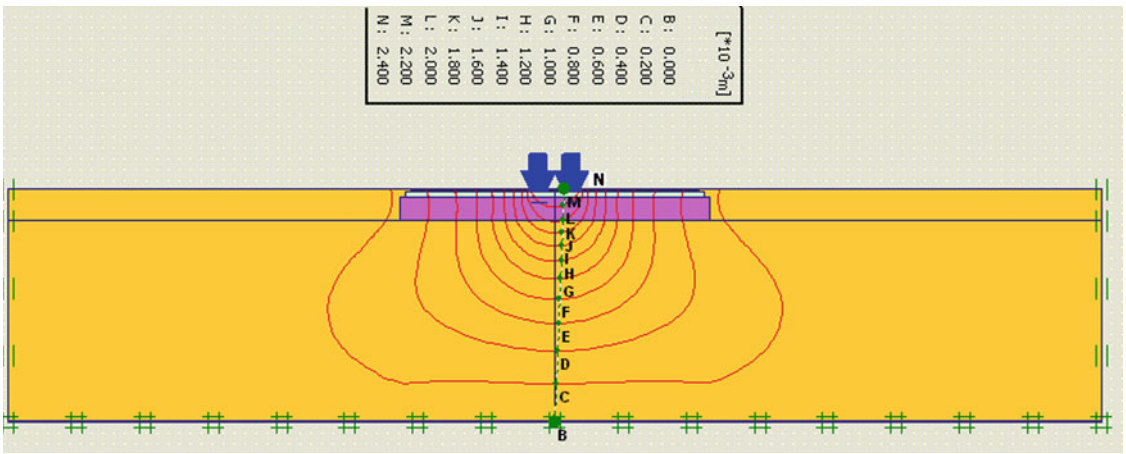

Fig. 10 Total settlement contours of U-PSL having $E = 80$ MPa

Table 7 Total settlement analyses' results for a 2-m thick C-PSL, if used instead of a 2-m thick U-PSL in a HSTR embankment

Layers	U-PSL	C-PSL						ASV (mm)	Notes
	ΔS_1 $E = 80$ MPa (mm)	ΔS_2 w/c = 0.4 C = 20 % $E = 352.9$ MPa (mm)	ΔS_3 w/c = 0.4 C = 25 % $E = 545.2$ MPa (mm)	ΔS_4 w/c = 0.4 C = 30 % $E = 597.5$ MPa (mm)	ΔS_5 w/c = 0.5 C = 20 % $E = 258.9$ MPa (mm)	ΔS_6 w/c = 0.5 C = 25 % $E = 261.5$ MPa (mm)	ΔS_7 w/c = 0.5 C = 30 % $E = 450.5$ MPa (mm)		
Ballast	1.993	0.401	0.253	0.231	0.552	0.542	0.309	<2	OK
Sub ballast	1.986	0.391	0.247	0.225	0.540	0.531	0.303	<2	OK
Prepared sub grade	1.875	0.377	0.240	0.219	0.518	0.512	0.293	<2	OK
Sub grade	1.598	0.345	0.219	0.197	0.475	0.467	0.268	<2	OK

ΔS_1 Plaxis-FEM calculated total settlement values, *ASV* allowable total settlement value [6])

$E = 80$ MPa value of U-PSL, as seen in Table 7 [12]. The obtained results showed that any such C-PSL mix can be used as a substitute of U-PSL.

2.1.5 Evaluation of the Results of Settlement Analyses

Results of settlement analyses via the Plaxis-FEM Program that was conducted on the 2-m thick uncemented-prepared-subgrade layer (U-PSL), for which the elasticity modulus value was taken as $E = 80$ MPa, is shown in Fig. 10 [12].

3 Discussion of the Results

Only three C-PSL mixes, having c = 20, 25, 30 % cement contents at w/c = 0.5, 0.4 water-to-cement ratios gave acceptable elasticity moduli higher than the required minimum value of $E = 80$ MPa of the U-PSL in a HSTR embankment [12]. For each of the six C-PSL mixes shown in Table 7, each layer was considered to have a thickness of 2-m in the analyses. Obtained E values were acceptable and much higher than the minimum required value of $E = 80$ MPa of U-PSL, meaning such a HSTR embankment will be much stiffer, a condition which is preferable. This means having a more durable embankment with a longer service life and less maintenance costs over long service life with less wear and tear for the train's undercarriage system (i.e. the wheel assembly) and for some of HSTR infrastructure, including slab-track, traverses, fasteners and rails. Alternatively, C-PSL thicknesses could be reduced proportionally, allowing some economy to be made in construction costs.

4 Conclusions

Results in Table 7 show the following:

The U-PSL in a typical HSTR embankment cross-section, such as shown in Fig. 1, can be replaced with any one of the listed C-PSL mixes. This will permit use of reduced layer thicknesses, while not exceeding the allowable settlement values (ASV). Using linear interpolation, simply this may mean that the original ($h = 2$ m) thickness of U-PSL can be replaced with $0.3h$-m high C-PSL at w/c = 0.5 (i.e. $h = 0.6$ m in thickness). Likewise, the original ($h = 2$ m) thickness of U-PSL can be replaced with $0.2h$ m high C-PSL at w/c = 0.4 (i.e. $h = 0.4$ m in thickness). Furthermore, the extra effort of doing in-situ soil compaction and testing in layers for U-PSL is reduced or eliminated. Generally speaking, it takes more volume of material, man-hours of work, time and cost to construct a U-PSL in a HSTR embankment to meet its minimum acceptable standards, compared to any one of the above described six mixes of C-PSL reduced in thicknesses in a HSTR embankment. In this way, HSTR embankment designers/constructors may have not only alternative methods, but also substantial savings in construction time and costs.

Acknowledgments This paper is based upon the postgraduate (M.Sc.) thesis study conducted at the Civil Engineering Department (CED) of the Izmir Institute of Technology-IzTech (http://www.iyte.edu.tr) in Urla-Izmir, Turkey. Also, the authors would like to express their gratitude to Asst. Prof. Dr. Ritchie Eanes for his careful proof-reading of the manuscript with patience.

References

1. UIC Report: High Speed Principles and Advantages. International Union of Railway, Paris (2007). http://www.uic.org
2. Seling, E.T.; Waters, J.M.: Track Geotechnology and Substructure Management. Thomas Telford Services Ltd., London (1994)
3. Chandra, S.; Agarwal, M.M.: Railway Engineering. Oxford University Press, New Delhi (2007)
4. Mundrey, J.S.: Railway Track Engineering, 3rd edn. Tata-McGraw-Hill PCL, New Delhi (2008)
5. UIC Code-719R: Earthworks and track-bed layers for railway lines. International Union of Railway, Paris (1994). http://www.uic.org
6. Egeli, I.: Design and Construction Aspects of High-Speed Train Railway Embankments—An Overview. Engineering Consultancy Report, THRC, Taiwan (2003)
7. TS 500: Betonarme Yapıların Hesap ve Yapım Kuralları, Türk Standardları Enstitüsü (in Turkish), Ankara (2000). http://www.tse.org.tr
8. TS 706: Beton Agregaları, Türk Standardları Enstitüsü (in Turkish), Ankara (2009). http://www.tse.org.tr
9. TS 802: Beton Karışımı Tasarım Hesap Esasları, Türk Standardları Enstitüsü (in Turkish), Ankara (2009). http://www.tse.org.tr
10. TS EN 12390-2: Laboratuvarda Dayanım Deneylerinde Kullanılacak Deney Numunelerinin Hazırlanması ve Kürlenmesi, Türk Standardları Enstitüsü (in Turkish), Ankara (2002). http://www.tse.org.tr
11. TS EN 12390-3: Deney Numunelerinde Basınç Dayanımının Tayini, Türk Standardları Enstitüsü (in Turkish), Ankara (2003). http://www.tse.org.tr
12. Usun, H.: Laboratory Study for Determining Geotechnical Engineering Properties of Cement-Treated and–Untreated Backfill Soils used in High Speed Railway Embankments, M.Sc. Thesis, Department of Civil Engineering, Izmir Institute of Technology, Izmir (2010). http://www.iyte.edu.tr
13. EN 1991-2: Eurocode 1: Actions on Structures—Part 2: Traffic Loads on Bridges, European Standard:CEN-Cenelec, Brussels (1991). http://www.cenelec.eu